Synergistic Effects of Sonolysis Combined with Ozonolysis for the Oxidation of Azobenzene and Methyl Orange

Hugo Destaillats, A. J. Colussi, Jiju M. Joseph, and Michael R. Hoffmann*

W. M. Keck Laboratories, California Institute of Technology, Pasadena, California 91125

Received: April 14, 2000; In Final Form: July 19, 2000

Most advanced oxidation processes (AOP) readily decolorize but are unable to mineralize aqueous azo dye solutions. The extent of mineralization—measured as total organic carbon (TOC) losses—during the 500-kHz sonication of azobenzene or methyl orange solutions increases from 20% to more than 80% in the presence of O_3. The abatement of the total organic load by the joint action of ultrasound and O_3 amounts to chemical synergism. Since TOC losses are not enhanced by ozonation followed by sonication and ground-state O atoms—that are produced by sonochemical O_3 thermolysis—are relatively unreactive, synergism likely involves the fast oxidation by ozone of free radical or unsaturated species generated by •OH radical attack on otherwise refractory products. Some of these products probably are saturated mono- and dicarboxylic acids, known to be resistant to O_3 oxidation. Nitrobenzene and benzoquinone, two rather persistent byproducts of sonolysis, are rapidly and completely mineralized by the combined oxidation treatment. Thus, direct ozonation of unsaturated sonolytic byproducts also accounts for part of the observed enhancement of the extent of mineralization. The anomalous kinetic behavior of the sonochemical degradation of benzoquinone (in the absence of O_3) is accounted for by its particularly high reactivity toward the relatively inert HO_2• and O_2^-• radicals.

Introduction

Azo dyes, which were designed to resist chemical and photochemical degradation, are relatively stable under normal wastewater treatment conditions. As a consequence, several advanced oxidation methods have been tested for their complete degradation, such as photolysis in the presence of H_2O_2,[1,2] TiO_2 photocatalytic oxidation,[3−6] Fenton's reaction,[7,8] radiolysis,[9] and ultrasonic irradiation.[10,11] These techniques decolorize the effluents, lowering dye concentration to sub-parts per million levels, but fail, however, to achieve a high degree of mineralization to CO_2. Recent changes in the Safe Drinking Water Act, which designate total organic carbon (TOC) as a nonspecific contaminant in drinking water, have created a demand for improved treatments.[12]

We recently reported on the sonochemical degradation of azobenzene and the azo dyes methyl orange, *o*-methyl red and *p*-methyl red in aqueous solutions saturated with inert gases.[11] Although full substrate degradation was normally attained in less than 30 min in each case, TOC levels remained at 50% for the dyes and at 70% for azobenzene after the first 2 to 3 h of irradiation.

Searching for ways to improve the organic carbon removal efficiency, we examined the combination of ultrasonic irradiation with ozonation, for the degradation of azobenzene (AB) and methyl orange (MO) in aqueous solution. When sonicated solutions are saturated with inert gases such as argon, most of the •H and •OH radicals generated in the core of cavitation bubbles recombine before reaching the solution.[13,14] Thus, a substantial portion of the mechanical energy required to produce cavitation is lost through recombination reactions such as the decomposition of water into •H and •OH, which in turn yield mainly H_2(g) and H_2O_2(aq), as well as reformation of H_2O. New reaction pathways, which improve the overall sonochemical energy efficiency by employing ozone (in mixtures with O_2) as background gas, are being elucidated.[15,16] In the case of volatile substrates such as methyl *tert*-butyl ether, MTBE, the observed enhancement in the extent of degradation can be accounted for by an enhanced oxidation in the cavitation bubbles. In the case of our present work, however, this mechanism does not apply to AB or MO, since their vapor pressures are negligible.

Despite an almost instantaneous decolorization of dye solutions upon ozonation, this method of oxidation is one of the less effective techniques for reducing TOC.[17,18] The more extensive mineralization, which is observed when these two techniques are combined, is evidence of a chemical synergism, in which dead-end byproducts of one process are efficiently degraded by the other. The actual concentration of O_3(aq) is drastically reduced upon sonication due to its decomposition in the cavitation bubbles and in solution.[19] Hence, new and more active oxygen species may also be produced and released into solution that replace O_3(aq) as primary oxidizing agents in the combined technique.

Experimental Section

The experimental setup employed in this study has been described elsewhere.[19] The sonochemical reactor consisted of a 650-mL glass chamber attached to a piezoelectric transducer, surrounded by a self-contained water jacket. Sonication at 500 kHz was performed with an ultrasonic transducer (Undatim Ultrasonics) operating at 50 W (2 W/cm^2). The ultrasonic power input to the reactor was determined using a standard calorimetric method.[20] The solution was stirred magnetically during each experiment, and the temperature was kept constant at 15.0 ±

* To whom correspondence should be addressed at the California Institute of Technology. Tel.: (626) 395-4391. Fax: (626) 395-3170. E-mail: mrh@cco.caltech.edu.

10.1021/jp001415+ CCC: $19.00 © 2000 American Chemical Society
Published on Web 09/08/2000

TABLE 1: Experimental Conditions for Ozone Generation

applied voltage	$[O_3(aq)]_{sat}/\mu M$	$[O_3(aq)]_{sat}^{US}/\mu M$	p_{O_3}/mbar
50	310	19	24
33	167	4.5	12.7
20	86	-	6.6
13	27	-	2.1

0.5 °C with a VWR Scientific thermostat. Variable O_3/O_2 ratio mixtures were produced in an Orec V10−O-804 generator by applying different voltages on a constant flow of O_2(g) at 1.5 bar. Oxygen gas was filtered through Drierite and a molecular sieve (Alltech) and through an activated charcoal hydrocarbon trap (Alltech) before being fed to the ozonator. The gaseous mixture was bubbled in the solution through a glass-fritted diffuser at a flow rate of 50 mL/min. Inert PTFE tubing was used throughout to preclude organic carbon contamination of the solutions resulting from O_3(g) attack of tubing walls, observed when other materials were employed.

Four different O_3/O_2 ratios (i.e., applied voltages) were used. In each case, the absorbance at 260 nm of the resulting ozone saturated aqueous solutions ($\epsilon = 3300\ M^{-1}\ cm^{-1}$) was determined using a Hewlett-Packard 8452-A diode array spectrophotometer. Similar measurements under ultrasound irradiation revealed extensive O_3 decomposition. The $[O_3(aq)]_{ss}$ saturation concentration in pure water for each voltage applied, with and without ultrasound irradiation, is reported in Table 1. The partial pressure of O_3(g), that is, the composition of the gas mixture, was calculated from the saturation values using the known Henry's constant,[21] $k_H^{O_3}$ (288 K) = 76.18 bar M^{-1}.

Aqueous solutions of AB and MO (10 μM) were prepared before each run and filtered through Millipore GS 0.22-μm disks. The same procedure was employed for the preparation of 20-μM solutions of the byproducts nitrobenzene (NB) and benzoquinone (BQ). Concentrations were determined spectrophotometrically ($\epsilon = 22000\ M^{-1}\ cm^{-1}$ at 319 nm for AB; $\epsilon = 26900\ M^{-1}\ cm^{-1}$ at 464 nm for MO; $\epsilon = 8852\ M^{-1}\ cm^{-1}$ at 266 nm for NB; and $\epsilon = 12589\ M^{-1}\ cm^{-1}$ at 250 nm for BQ). The pH of the solutions was measured using an Altech 71 pHmeter.

Samples were collected for analysis at different times through a septum port by means of a glass syringe. The UV−vis absorption spectra of the reaction mixture were recorded as a function of time using a conventional semi-micro quartz cuvette with a 10-mm path length. Total organic carbon analyses were carried out with a Shimadzu 5000A TOC analyzer operating in the nonpurgable organic carbon (NPOC) mode. When needed, samples collected for TOC analysis were inmediately quenched with 1 mL $Na_2S_2O_3$ 0.07 M to scavenge the residual O_3 and preserve sample composition prior to the analysis. Each sample was measured at least 3 times; the reported result is the averaged value. The experimental error was calculated in each case from the dispersion of the data, being always ≤10% of the reported value. Product analysis by HPLC-ES-MS was described previously.[11] Calculations were performed with Mathematica 4.0.[22]

MO (Baker, >95%), AB (Aldrich, >99%), NB (Aldrich, 99%), BQ (Sigma, >99%), and $Na_2S_2O_3$ (EM, >99%) were used without further purification. The solutions were prepared using water purified by a Millipore Milli-Q UV Plus system (R = 18.2 MΩ.cm). O_2(g) was provided by Air Liquide.

Results and Discussion

Enhanced Mineralization. Figures 1 and 2 summarize the results obtained when either ultrasound, ozonation, or their combination was applied to AB and MO solutions, respectively.

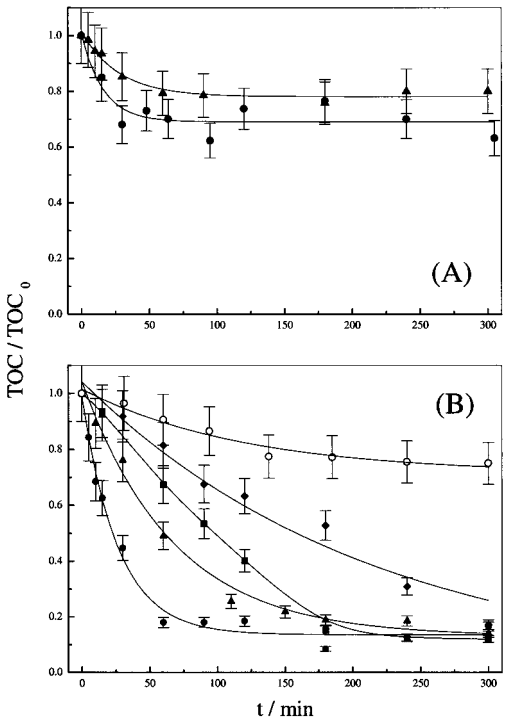

Figure 1. Mineralization of azobenzene solutions at 15 °C and pH = 6.5 to 5.5: (A) ozonation only and (B) with ultrasonic irradiation at 500 kHz. Applied voltage at the ozone generator: ●, 50 V; ▲, 33 V; ■, 20 V; ◆, 13 V; and ○, without ozone.

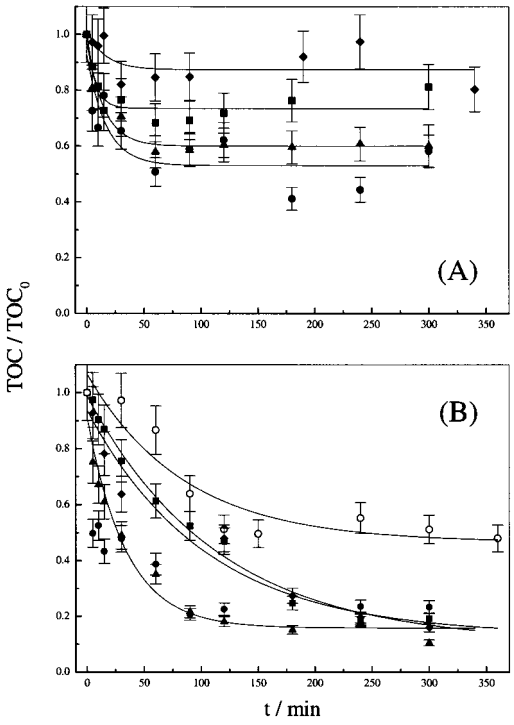

Figure 2. Mineralization of methyl orange solutions at 15 °C and pH = 6.5 to 5.5: (A) ozonation only and (B) with ultrasonic irradiation at 500 kHz. Applied voltage at the ozone generator: ●, 50 V; ▲, 33 V; ■, 20 V; ◆, 13 V; and ○, without ozone.

The use of ultrasound alone on AB led to a limiting mineralization of about 20% after 150 min (Figure 1B, open circles). Similarly, ozone alone could only reduce TOC by about 30%, that is, $TOC_\infty \cong 0.7\ TOC_0$, even at the highest O_3/O_2 ratios (Figure 1A). In contrast, when the combined agents were employed, the extent of mineralization exceeded 80% at all O_3 concentrations (Figure 1B), although TOC_∞ was reached sooner

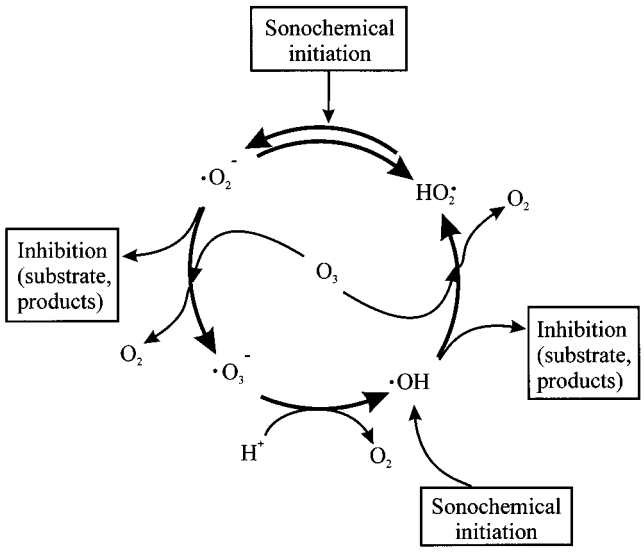

Figure 3. Initiation, promotion, and inhibition of the decomposition of O_3(aq) under ultrasonic irradiation.

at the higher O_3/O_2 ratio mixtures. Similar results were observed with MO as a substrate (Figure 2). In this case, ozonation or sonication led to about 50% TOC reductions, but their combination achieved a faster and more complete mineralization, with $TOC_\infty \leq 0.2\ TOC_0$.

We recently reported the qualitative product analysis of the sonochemical degradation of AB and MO performed by HPLC-ES-MS.[11] Some relatively stable aromatic compounds were observed among the main byproducts. In contrast, no aromatic products could be detected as sonolytic byproducts by using ozone as a background gas. Since most concentrations were near the detection limit of the ES-MS, we were not able to identify the remaining products in the latter case. ES-MS also proved to be a poor method for identifying the main products of ozonation. Nevertheless, the complete absence of NO_3^- ($m/z = 62$) or of aromatic compounds suggests that ozonation and sonication proceed by very different pathways. The reactivity of O_3 toward activated aromatic rings is higher or at least similar to that observed toward azo double bonds.[21,23] Thus, the cleavage of the N=N bond cannot be considered the primary degradative step in the case of ozonolysis, as opposed to what we observed during sonolysis under inert gases.

To verify the refractory nature of AB ozonation products, we performed a sequential ozonation−sonolysis treatment. After a 60-min ozonation (at 33 V) of a 10-μM AB solution, which is sufficient to achieve the maximum possible effects, ultrasonic irradiation under O_2 for 200 min was unable to further reduce TOC levels. This fact underscores the importance of the apparent chemical synergism operating when sonolysis is combined with ozonolysis. The combined action must involve the fast oxidation by ozone of the free organic radicals produced in the •OH radical attack on otherwise refractory species. The latter species appear to be partially oxidized, saturated mono- and dicarboxylic acids that are known to be resistant both to ozonation and ultrasonic irradiation performed separately.

Aqueous Ozone Chemistry under Ultrasonic Irradiation. When sonicated liquids are bubbled with O_3/O_2 mixtures, the thermal decomposition of O_3(g) in the cavitation bubbles leads to enhanced •OH radical and H_2O_2 yields. In the vapor phase of cavitation bubbles, reaction 1

$$O_3(g) \rightarrow O_2(g) + O(^3P)(g) \qquad (1)$$

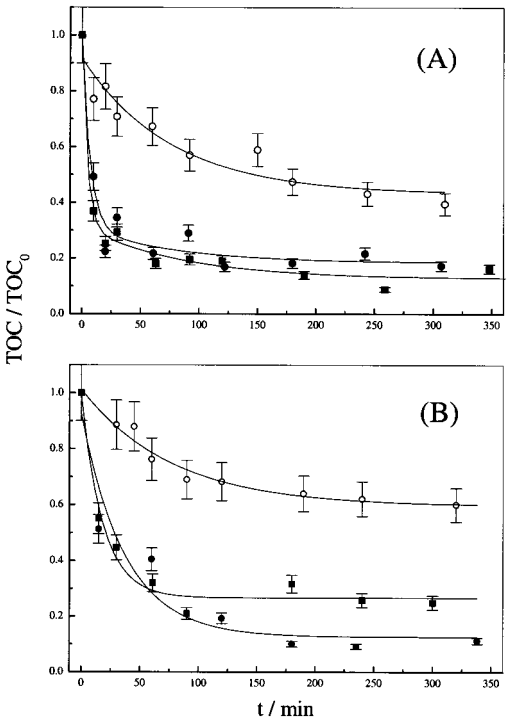

Figure 4. (A) Mineralization of benzoquinone solutions at 15 °C and pH = 6.5 to 5.5. (B) Mineralization of nitrobenzene solutions at 15 °C and pH = 6.5 to 5.5. ○, ultrasonic irradiation under O_2 atmosphere; ■, ozonation (50 V); and ●, combined sonolysis/ozonolysis (similar experimental conditions).

proceeds at relatively low temperatures, as compared with the more extreme values needed to decompose solvent molecules upon bubble collapse. Hence, the cavitation bubbles that are able to decompose ozone under mild conditions at a given time are more numerous than those reaching temperatures high enough to dissociate the H_2O molecule. Although the ground-state O atoms produced are rather unreactive and mostly recombine to yield O_2, they also contribute to increase the •OH radical (and their recombination product, H_2O_2) production by cavitation bubbles through the reaction

$$O(^3P)(g) + H_2O(g) \rightarrow 2\ \bullet OH(g) \qquad (2)$$

In the aqueous phase, the remaining dissolved ozone may react directly with the target substrates and their initial degradation byproducts or with the species originating during water (and ozone) sonolysis, as follows:[21]

$$\bullet OH + O_3 \rightarrow \bullet HO_2 + O_2 \qquad k_3 = 1.1 \times 10^8 \qquad (3)$$

$$\bullet O_2^- + O_3 \rightarrow O_2 + \bullet O_3^- \qquad k_4 = 1.5 \times 10^9 \qquad (4)$$

$$\bullet O_3^- + H^+ \rightarrow \bullet OH + O_2 \qquad k_5 = 9.0 \times 10^9 \qquad (5)$$

$$H_2O_2 + O_3 \rightarrow \bullet OH + \bullet HO_2 + O_2 \qquad k_6 = 0.025 \qquad (6)$$

Even though the decomposition of ozone as catalyzed by OH^- is slow and can be neglected over the pH range of this study,[24] the chain reaction process of eqs 3−6 appears to be activated under ultrasonic irradiation, as illustrated in Figure 3. Therefore, the major part of the dissolved ozone is efficiently decomposed by ultrasonic irradiation (Table 1). In the combination of sonolysis and ozonolysis, the substrates and their byproducts are able to react either with O_3(aq) or with one of the active

TABLE 2: Reported Rate Constants for Reactions of the Substrates and Some of the Main Degradation Byproducts with •OH(aq), O_3(aq), and • HO_2(aq)/•O_2^-(aq) in Water at Room Temperature

	•OH $k_i^{OH}/M^{-1}\ s^{-1}$	O_3 $k_i^{O_3}/M^{-1}\ s^{-1}$	•HO_2/•O_2^- $k_i^{HO_2}/M^{-1}\ s^{-1}$	ref
azobenzene	2×10^{10}	220		26, 27
methyl orange	2×10^{10}			28
nitrobenzene	3.9×10^9	0.09		29, 30
benzene sulfonate	4.7×10^9	0.23		29, 30
phenol	1.8×10^{10}	1300		29, 30
catechol	1.1×10^{10}	2.86×10^5	$4.7 \times 10^4/2.7 \times 10^5$	31, 30, 32
nitrophenol	3.8×10^9	<50		33, 30
hydroquinone	2.1×10^{10}	1.43×10^6	$8.5 \times 10^3/1.7 \times 10^7$	31, 30, 34, 32
benzoquinone	1.2×10^9		$/1.0 \times 10^9$	30, 34, 32
oxalate	7.7×10^6	<0.04	/<0.20	33, 30, 32
hydrogen oxalate	4.7×10^7			30
maleic acid	6×10^9	1000	/<0.06	33, 30, 32
formic acid	1.3×10^8	5		33, 30
formate	3.5×10^9	100	/<0.01	33, 30, 32
formaldehyde	1×10^9	0.1		29, 30

species generated by the combined sonolysis of water and ozone, thus providing new alternative degradative pathways. The presence of a variety of reactive radicals, particularly at the beginning of the degradation process, may also drive the reaction toward the production of more single-ring aromatic intermediates, as observed during sonolysis in our previous work.[11] The latter, as we will illustrate below, can be then easily degraded by O_3(aq) and by the radical intermediates as well, providing an effective pathway towards mineralization.

Probing Sonolytic Byproducts. Two relatively stable byproducts of sonochemical degradation were selected as probes to investigate the effect of ozone in sonolysis: nitrobenzene (NB) and benzoquinone (BQ). Figure 4 illustrates the mineralization of NB and BQ aqueous solutions at 15 °C in the pH range 6.5 to 5.5 for ultrasonic irradiation under an O_2 atmosphere, ozonation at 50 V, and combined sonolysis/ozonolysis in similar experimental conditions. The data in Figure 4 show that the high reactivity of NB and BQ toward ozone, under the conditions of our experiment, may account, in part, for the increased extent of mineralization and the reaction rates observed with AB and MO. In contrast, almost no appreciable improvement results from the sonication of solutions that had previously (or simultaneously) undergone simple ozonation. The combined technique in these cases (particularly for BQ) yielded almost the same results as ozonation alone. Furthermore, these results suggest that the persistent species in ozonation are chemically different from those produced by sonication, since some of the latter are readily degraded by O_3(aq).

The relative stability of BQ and NB under ultrasonic irradiation in the absence of ozone is consistent with their relative inertness to •OH(aq) radicals, as compared with the precursor dyes substrates, and with most of the other byproducts generated during the reaction. Table 2 summarizes the relevant rate constants reported for the reactions of AB, MO, and some byproducts of their degradation, with •OH(aq), O_3(aq) and •HO_2-(aq)/•O_2^-(aq). In the case of BQ, the reaction with •OH is nearly 20 times slower than that of any of the substrates and is even slower than that of NB. The fact that the ultrasonic mineralization of BQ is slightly more efficient than that of NB, despite their relative k_i^{OH} values, is intriguing and may be related to the high reactivity of BQ toward superoxide (a poor oxidant in most other cases; see Table 2).

Role of •HO_2 and •O_2^- in the Sonolysis of BQ. When the sonochemical degradation of BQ and NB (without O_3) was followed spectrophotometrically, as shown in Figure 5, two completely different concentration versus time profiles were observed. The pseudo-first-order rate constants (k_i) for the

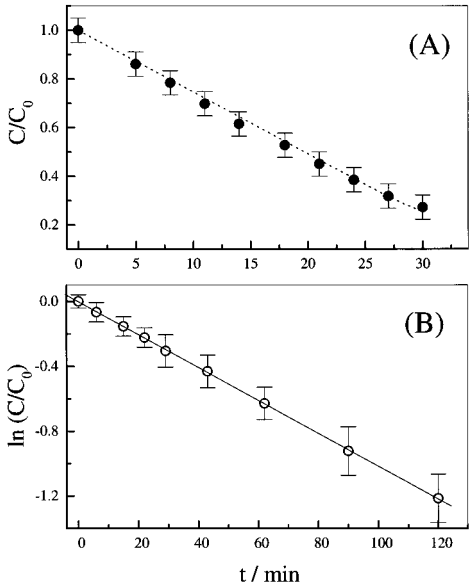

Figure 5. (A) Sonochemical degradation of benzoquinone at 15 °C and pH = 6.5 to 5.5. The experimental values (●) were reproduced by numerically solving eqs 17−20 (dashed line). (B) Sonochemical degradation of nitrobenzene at 15 °C and pH = 6.5 to 5.5. The experimental values (○) were adjusted using eq 7 (solid line).

TABLE 3: Pseudo-First-Order Rate Constants for the Sonochemical Degradation of Azobenzene, Methyl Orange, Nitrobenzene, and Benzoquinone under O_2 Saturation and Estimated Steady-State •OH Radical Concentration, $[•OH]_{ss}$

X	k_X/min^{-1}	$[•OH(aq)]_{ss}/M$
MO	0.042	3.5×10^{-14}
AB	0.043	3.6×10^{-14}
NB	0.010	4.4×10^{-14}
BQ	0.041	3.4×10^{-11}

sonochemical degradation of NB and BQ under O_2 saturation were estimated from these data and are reported in Table 3 together with those of AB and MO that were previously reported.[11] Assuming that •OH radicals are the only reactive species generated during sonolysis in the absence of O_3, the pseudo-first-order rate constants k_X,

$$\frac{d[X]}{dt} = k_X[X] \tag{7}$$

where X is any of the considered substrates (AB, MO, NB, or BQ), should include the steady-state concentration of •OH(aq), as follows:

$$k_X = k_X^{OH}[\bullet OH]_{ss} \quad (8)$$

Table 3 includes the calculated $[\bullet OH]_{ss}$ in the four cases, employing k_i^{OH} values from Table 2. Except for the value of BQ, which were estimated from the initial data points only, a good agreement exists in all other cases, thus providing a reasonable estimation for $[\bullet OH]_{ss}$. The deviation of BQ from the assumptions in the simple model of eq 1 becomes even more evident from the graphical representation (see Figure 5A). In this case, the process is not pseudo-first-order in [BQ] but rather zero order. Here, we should also consider the contribution of reactions of BQ with $\bullet HO_2$(aq) and, particularly at the working pH, of $\bullet O_2^-$(aq). The concentrations of these two species in solution increase with the irradiation time, since they originate in the reaction of the two main products of water sonolysis, •OH and H_2O_2, in the bulk liquid phase at room temperature:

$$\bullet OH(aq) + H_2O_2(aq) \rightarrow \bullet HO_2(aq) + H_2O \qquad k_9 = 2.7 \times 10^7 \quad (9)$$

$$\bullet HO_2(aq) \rightleftharpoons \bullet O_2^-(aq) + H^+(aq) \qquad pK_a = 4.8 \quad (10)$$

While •OH(aq) reaches a steady-state concentration, H_2O_2(aq) accumulates in the aqueous phase, thus increasing the production rate of superoxide with reaction time. Given the pH range of our experiment, the superoxide anion is the prevalent species, although $[\bullet HO_2]$ must also be appreciable.

To assess the role of $\bullet HO_2$(aq) and $\bullet O_2^-$(aq) in the depletion of BQ, a simple kinetic model is postulated in order to reproduce the experimental observations. The sonochemical production rates of •OH(aq) and H_2O_2(aq) under the same ultrasonic frequency and applied power were previously determined as $k_{OH} = 5.5 \times 10^{-9}$ M s^{-1} and $k_{H_2O_2} = 2.4 \times 10^{-8}$ M s^{-1}, respectively.[11] The relatively small generation of $\bullet HO_2$ in high-temperature gas-phase reactions during cavitation was neglected for simplicity, according to the observations by Hart and Henglein.[25] The model includes the reactions of BQ(aq) with •OH(aq) and $\bullet O_2^-$(aq) (eqs 11−12)

$$BQ(aq) + \bullet OH(aq) \rightarrow \text{products} \qquad k_{11} = 1.2 \times 10^9 \quad (11)$$

$$BQ(aq) + \bullet O_2^-(aq) \rightarrow \text{products} \qquad k_{12} = 1.0 \times 10^9 \quad (12)$$

and the radicals recombination processes of eqs 13−16 as follows:

$$2\bullet OH \rightarrow H_2O_2 \qquad k_{13} = 6 \times 10^9 \quad (13)$$

$$\bullet OH + \bullet O_2^- \rightarrow HO^- + O_2 \qquad k_{14} = 1.01 \times 10^{10} \quad (14)$$

$$\bullet HO_2 + \bullet O_2^- + H^+ \rightarrow H_2O_2 + O_2 \qquad k_{15} = 9.7 \times 10^7 \quad (15)$$

$$2\bullet HO_2 \rightarrow H_2O_2 + O_2 \qquad k_{16} = 8 \times 10^5 \quad (16)$$

The corresponding differential equations (eqs 17−20) describe the evolution of the species concentrations in the aqueous phase during continuous ultrasonic irradiation under O_2 saturation. We assume a complete deprotonation of $\bullet HO_2$(aq) to simplify the reaction scheme (i.e., $\bullet O_2^-$ is the only species considered in the calculations). The direct oxidation of BQ by H_2O_2 is a slow process that can be neglected under the present experimental conditions.

$$\frac{d[\bullet OH]}{dt} = k_{OH} - k_{11}[BQ][\bullet OH] - k_9[H_2O_2][\bullet OH] - 2k_{13}[\bullet OH]^2 - k_{14}[\bullet O_2^-][\bullet OH] \quad (17)$$

$$\frac{d[H_2O_2]}{dt} = k_{H_2O_2} + k_{13}[\bullet OH]^2 - k_9[\bullet OH][H_2O_2] \quad (18)$$

$$\frac{d[\bullet O_2^-]}{dt} = k_9[H_2O_2][\bullet OH] - k_{12}[BQ][\bullet O_2^-] - k_{14}[\bullet O_2^-][\bullet OH] - k_{15}[\bullet O_2^-]^2 \quad (19)$$

$$\frac{d[BQ]}{dt} = -k_{11}[BQ][\bullet OH] - k_{12}[BQ][\bullet O_2^-] \quad (20)$$

Although the reported values for the rate constants were determined between 20 °C and 25 °C, the temperature dependence of these diffusion-controlled rates is quite small. The dotted line in Figure 5A represents the calculated BQ depletion rate, and it shows a good agreement with the experimental values. The deviation from the simple pseudo-first-order model from eq 7 can thus be explained simply by the major contribution of superoxide in the BQ degradation (not observed for the other three substrates). This fact reveals the importance of considering, at least in some cases, a more complex scheme of reactions, considering the particular chemical nature of the species involved.

Acknowledgment. Financial support provided by the Department of Energy (DOE 1963472402) and the U.S. Navy (N 47408-99-M-5049) is gratefully acknowledged. J.M.J. thanks the ICSC World Laboratory for a research fellowship.

References and Notes

(1) Ince, N. *Water Res.* **1999**, *33*, 1080−1084.
(2) Shu, H.; Huang, C.; Chang, M. *Chemosphere* **1994**, *29*, 2597−2607.
(3) Nasr, C.; Vinodgopal, K.; Fisher, L.; Hotchandani, S.; Chattopadhyay, A.; Kamat, P. *J. Phys. Chem.* **1996**, *100*, 8436−8442.
(4) Vinodgopal, K.; Wynkoop, D.; Kamat, P. *Environ. Sci. Technol.* **1996**, *30*, 1660−1666.
(5) Lagrasta, C.; Bellobono, I.; Bonardi, M. *J. Photochem. Photobiol., A* **1997**, *110*, 201−205.
(6) Chen, L.; Chou, T. *J. Mol. Catal.* **1993**, *85*, 201−214.
(7) Tang, W.; Chen, R. *Chemosphere* **1996**, *32*, 947−958.
(8) Spadaro, J.; Isabelle, L.; Renganathan, V. *Environ. Sci. Technol.* **1994**, *28*, 1389−1393.
(9) Ravishankar, D.; Raju, B. *J. Radioanal. Nucl. Chem.* **1994**, *178*, 351−357.
(10) Vinodgopal, K.; Peller, J.; Makogon, O.; Kamat, P. *Water Res.* **1998**, *32*, 3646−3650.
(11) Joseph, J.; Destaillats, H.; Hung, H.; Hoffmann, M. *J. Phys. Chem A* **2000**, *104*, 301−307.
(12) Tseng, T.; Edwards, M. *J. AWWA* **1999**, *91*, 159−170.
(13) Colussi, A.; Weavers, L.; Hoffmann, M. *J. Phys. Chem. A* **1998**, *102*, 6927−6934.
(14) Hua, I.; Hoffmann, M. *Environ. Sci. Technol.* **1997**, *31*, 2237−2243.
(15) Kang, J.; Hoffmann, M. *Environ. Sci. Technol.* **1998**, *32*, 3194−3199.
(16) Kang, J.; Hung, H.; Lin, A.; Hoffmann, M. *Environ. Sci. Technol.* **1999**, *33*, 3199−3205.
(17) Sarasa, J.; Roche, M.; Ormad, M.; Gimeno, E.; Puig, A.; Ovelleiro, J. *Water Res.* **1998**, *32*, 2721−2727.
(18) Peralta-Zamora, P.; Kunz, A.; de Moraes, S.; Pelegrini, R.; Moleiro, P.; Reyes, J.; Duran, N. *Chemosphere* **1999**, *38*, 835−852.
(19) Weavers, L.; Hoffmann, M. *Environ. Sci. Technol.* **1998**, *32*, 3941−3947.
(20) Mason, T. J. *Practical Sonochemistry: User's Guide to Applications in Chemistry and Chemical Engineering*; Ellis Horwood: London, 1991.
(21) Langlais, B.; Reckhow, D. A.; Brink, D. R. *Ozone in Water Treatment. Application and Engineering*; Lewis Pub. Inc.: Denver, 1991.

(22) Wolfram, S. *Mathematica*; Wolfram Media and Cambridge University Press: Cambridge, 1996.
(23) Bailey, P. *Ozonation in Organic Chemistry*; Academic Press: New York, 1982; Vol. 2.
(24) Hoigne, J.; Bader, H. *Water Res.* **1976**, *10*, 377−386.
(25) Hart, E.; Henglein, A. *J. Phys. Chem.* **1985**, *89*, 4342−4347.
(26) Yao, C.; Haag, W. *Water Res.* **1991**, *25*, 761−773.
(27) Panajkar, M.; Mohan, H. *Indian J. Chem., Sect. A* **1993**, *32*, 25−27.
(28) Padmaja, S.; Madison, S. *J. Phys. Org. Chem.* **1999**, *12*, 221−226.
(29) Hoigne, J.; Bader, H. *Water Res.* **1983**, *17*, 173−183.
(30) Buxton, G.; Greenstock, C.; Helman, W.; Ross, A. *J. Phys. Chem. Ref. Data* **1988**, *17*, 513−886.
(31) Gurol, M.; Nekouinaini, S. *Ind. Eng. Chem. Fundam.* **1984**, *23*, 54−60.
(32) Bielski, B.; Cabelli, D.; Arudi, R.; Ross, A. *J. Phys. Chem. Ref. Data* **1985**, *14*, 1041−1100.
(33) Hoigne, J.; Bader, H. *Water Res.* **1983**, *17*, 185−194.
(34) Rao, P. S.; Hayon, E. *J. Phys. Chem.* **1975**, *79*, 397.